AIP Conference Proceedings

A new contact model for modelling of elastic-plastic-adhesive spheres in distinct element method

Massih Pasha, Selasi Dogbe, Colin Hare, Ali Hassanpour, and Mojtaba Ghadiri

Citation: AIP Conf. Proc. **1542**, 831 (2013); doi: 10.1063/1.4812060
View online: http://dx.doi.org/10.1063/1.4812060
View Table of Contents: http://proceedings.aip.org/dbt/dbt.jsp?KEY=APCPCS&Volume=1542&Issue=1
Published by the AIP Publishing LLC.

A New Contact Model for Modelling of Elastic-Plastic-Adhesive Spheres in Distinct Element Method

Massih Pasha, Selasi Dogbe, Colin Hare, Ali Hassanpour and Mojtaba Ghadiri

Institute of Particle Science and Engineering, University of Leeds, Leeds, UK

Abstract. Rigorous models of elasto-plastic contact deformation are time-consuming in numerical calculations for the Distinct Element Method and quite often unnecessary to represent actual contact deformation of common particulate systems. In this work a simple linear elastic-plastic-adhesive contact model for spherical particles is proposed, whereby the loading cycle is a linear plastic deformation and the unloading is elastic with a higher stiffness compared to the plastic deformation. The adhesive behaviour is considered once the unloading contact force reaches the pull-off force, at which point the contact deforms with negative elastic-adhesive stiffness. In order to account for increase in adhesion due to plastic deformation, the pull-off force is evaluated using negative linear plastic-adhesive stiffness. The model is applied to compression of spherical particles with elastic-plastic-adhesive contacts for which sensitivity analyses of the model parameters on work of compaction are carried out. As the ratio of elastic to plastic stiffness is increased, the plastic component of the total work increases for a given strain and the elastic component decreases. Large stiffness ratio values imply particles undergoing larger plastic work for a given strain. By increasing interface energy, the plastic work increases for a given solid fraction, however the elastic work does not change. In this case, the maximum tensile force is increased therefore the work of adhesion is increased.

Keywords: DEM, Molecular dynamics (MD) and discrete element model (DEM) force-laws, Cohesive powder, Plastic deformation, Adhesion.
PACS: 46.55.+d "Adhesion: mechanical contacts (structural mechanics)"

INTRODUCTION

The macroscopic bulk behaviour of powders is governed by the microscopic activity of the individual particles in an assembly. This implies that in order to gain a better understanding of particulate systems and their functioning, the particle interactions at the microscopic level must be analysed. It is currently very difficult to investigate the behaviour of individual particles within a bulk assembly experimentally. Therefore it is helpful to model the behaviour of particles by the use of numerical simulation. For particulate solids, the most appropriate approach for this purpose is the use of computer simulation by the Distinct Element Method (DEM). Considering a wide range of factors involved in the interactions, modelling of inter-particle contacts is particularly a complex process. Various contact models have been developed in the literature for elastic, elastic and adhesive, elasto-plastic and elasto-plastic and adhesive contacts, most of which involve complex mathematical equations. The complexity of these models makes their implementation in the computer codes difficult and would result in slower simulations. Simplifications can be done in order to reduce the computational complexity of the models; however this would come at the expense of losing the accuracy of capturing the realistic behaviour. In the present work a linear model is proposed based on improvements of Luding's model [1] by considering aspects of Thornton and Ning's [2] and Tomas's [3] models. Sensitivity analyses of the proposed model parameters on bulk compaction behaviour were also investigated.

LUDING'S ELASTO-PLASTIC AND ADHESIVE CONTACT MODEL

Figure 1 illustrates schematically the normal contact model of Luding [1] for elasto-plastic and adhesive contacts.

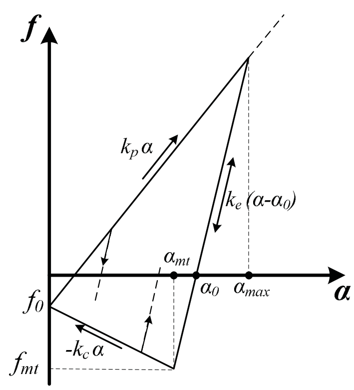

FIGURE 1. Schematic diagram of force-overlap relationship in Luding's [1] model.

Powders and Grains 2013
AIP Conf. Proc. 1542, 831-834 (2013); doi: 10.1063/1.4812060

In this model, the normal force will immediately drop to a certain negative value, f_0, when two spheres come into contact due to van der Waals attractive forces [2, 4]. On initial compression loading, the contact is considered to be plastically deforming; the contact force increases linearly with the overlap α, until an overlap α_{max} is reached (α_{max} is kept in memory as a history variable). The line with slope k_p thus defines the maximum force possible for a given α. During unloading the force drops on a line with slope k_e. The force decreases to zero at overlap α_0, which represents the plastic contact deformation. Reloading at any instant leads to an increase of the force along the same line with slope k_e, until the previous maximum force is reached; if α increases further beyond α_{max}, the force again follows the line with slope k_p and α_{max} has to be adjusted accordingly. Unloading below α_0 produces an adhesive force until the maximum tensile force, f_{mt}, is reached at the overlap α_{mt}. Further unloading leads to a reduction in attractive forces on the adhesive branch with slope $-k_c$. The maximum tensile force in this model increases by having larger deformations, i.e. increasing α_{max} would result in a larger negative f_{mt}. This behavior is in line with the model of Thornton and Ning [2], where the pull-off force required to overcome the adhesion increases with the impact velocity due to the locally increased radius of curvature. Luding's model contains two functional flaws by which the behaviour of elasto-plastic and adhesive contacts is not realistically simulated. First, contacts break at zero overlap ($\alpha = 0$), regardless of loading or unloading history. This implies that all plastic deformation has been recovered, which is unrealistic since plastic deformation is permanent. The second issue is with the reloading behaviour at overlaps smaller than α_{mt}, where reloading follows a linear line parallel to the initial unloading curve. Since the contact unloading is considered to be elastic, the reloading at any point must follow unloading curve up to the point unloading began (α_{max}). For further loading beyond this point, the force should follow the line with slope k_p. In the case of elasto-plastic contacts with no adhesion, the contact force starts from zero (i.e. $f_0 = 0$) and the cohesive stiffness is zero (i.e. $f_{mt} = 0$).

PROPOSED CONTACT MODEL

The proposed model offers an improvement over Luding's model by considering aspects of Thornton and Ning's [2] and Tomas's [3] elasto-plastic and adhesive models, but adapting linear profiles for loading and unloading. Adhesive detachment of a contact with plastic deformation occurs at a finite value of overlap, α_p, rather than at $\alpha = 0$ as in Luding's model. To account for this, an elastic-adhesive stiffness, k_{ce}, is considered for unloading of the contact for overlaps smaller than α_{mt}, as can be seen schematically in Figure 2.

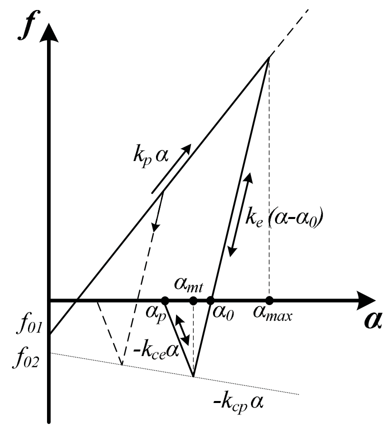

FIGURE 2. Schematic diagram of the normal force-overlap relationship in the proposed model.

The initial contact force, f_{01}, is considered to be equal to the elastic JKR pull-off force [4] as indicated by Equation 1.

$$f_{01} = \frac{3}{2}\pi R^* \Gamma \tag{1}$$

where R^* is the reduced radius given by Equation 2 and Γ is the interface energy.

$$R^* = \left(\frac{1}{R_1} + \frac{1}{R_2}\right)^{-1} \tag{2}$$

where R_1 and R_2 are the radii of the spheres in contact. The increase in the pull-off force due to increased plastic deformation in this model is governed by the plastic-adhesive stiffness, k_{cp} (see Figure 2). The value of f_{02} in the model (see Figure 2) is governed by adhesion in the plastic contact area. The reloading in the proposed model follows first the unloading lines ($-k_{ce}\alpha$) for overlaps smaller than α_{mt} and then $k_e(\alpha\text{-}\alpha_0)$ for overlaps larger than α_{mt} since the unloading is assumed to be purely elastic [2]. However once during the reloading the overlap reaches α_{max}, the contact starts deforming plastically again and the force is calculated by $k_p\alpha$. In the case of cohesionless contacts, the loading-unloading behaviour becomes identical to Luding's model [1]. However, in contrast to Luding's model, reloading at overlaps smaller than α_0 is not possible (the force is zero up to α_0).

SENSITIVITY ANALYSIS OF THE PROPOSED MODEL PARAMETERS

A set of simulations were carried out in order to investigate the effects of the model parameters on the elastic and plastic components of work during loading and unloading of bulk compression. The proposed model was implemented as a subroutine for EDEM® software provided by DEM-Solutions, Edinburgh, UK. The tangential stiffness, k_t, was equated to the elastic stiffness, k_e, throughout the simulations. The model parameters for the particles are summarised in Table 1.

TABLE 1. Model parameter values used in the simulations.

Property	Value range
Elastic stiffness, k_e (kN/m)	1-5000
Plastic stiffness, k_p (kN/m)	1-2500
Interface energy, Γ (J/m^2)	0-5

The walls were considered to be elastic with zero adhesion (i.e. $f_{01} = f_{02} = 0$, $k_{ce} = k_{cp} = 0$ and $k_p = k_e = k_t$). The stiffness of the walls was set to be 8000 kN/m. 3400 particles with a mean diameter of 1 mm and a normal size distribution with standard deviation of 0.095 mm were generated inside a cylindrical die of 12 mm diameter. This number of particles provided a bed height of approximately 36 mm. The density of the particles was set to be 1000 kg/m^3.

The compression was simulated at a strain rate of 0.28 s^{-1}. The process is therefore within the quasi-static regime, hence the inertial effects are minimised [5]. The assembly was compressed by moving the top platen until a bulk strain of 11% (for non-cohesive cases) or a solid fraction of 0.58 (for cohesive cases) was achieved, after which the platen was unloaded with the same speed as the compression. Figure 3 shows a typical force-displacement curve of the top platen during the bulk compression using DEM.

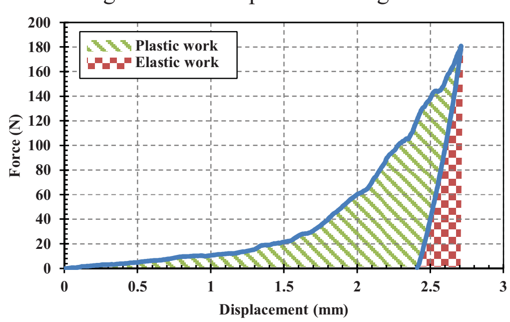

FIGURE 3. Typical loading-unloading curve of compaction.

The plastic work on loading is calculated as the closed area underneath the curve. The elastic work is calculated as the area underneath the unloading curve. The total input work is the addition of the plastic and elastic work components. The normalised elastic and plastic work component are defined as the elastic and plastic work, respectively, divided by the input work.

RESULTS AND DISCUSSION

Figure 4 shows the normalised elastic and plastic work components as a function of stiffness ratio, k_e/k_p, for all the cohesionless cases.

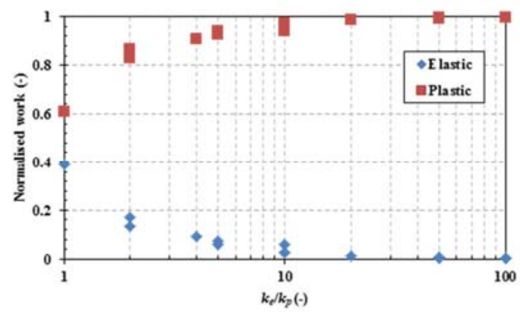

FIGURE 4. Normalised work as a function of stiffness ratio for all the cohesionless cases.

Large stiffness ratio values imply particles deforming extensively plastically, whereas a stiffness ratio of one implies a purely elastic deformation. For the stiffness ratio of one, the plastic component of the work is still larger than the elastic one. The plastic work has only contributed towards particle rearrangements and frictional forces between the particles and with the walls, since the contacts deform elastically. The graph shows that as the stiffness ratio increases, the fraction of plastic work increases, while that of elastic work decreases. The increase in the ratio means either the plastic stiffness is decreased or the elastic stiffness is increased. If the plastic stiffness is decreased while the elastic stiffness is kept constant (softer particles), more work is expended in deforming contacts to reach the same force. This leads to an increase of the total work, while the elastic work remains the same. Therefore normalised elastic work decreases and normalised plastic work increases. In the case where the elastic stiffness is increased while plastic work is kept constant, the total input work does not change, but the fraction of elastic work decreases. This leads to a decrease in the normalised elastic work and consequently normalised plastic work increases. It can also be seen from Figure 4 that there exists a limit for the stiffness ratio ($k_e/k_p \approx 20$) beyond which almost all of the work input into the system is used in plastic deformation.

Figure 5 shows the plastic and elastic works as a function of increasing the interface energy.

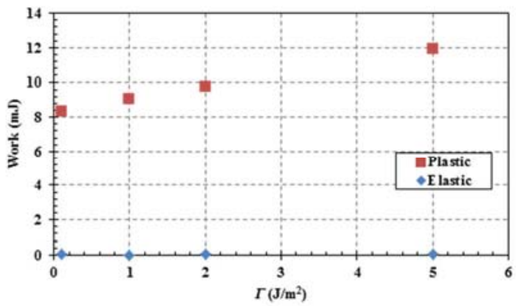

FIGURE 5. Elastic and plastic work components as a function of Γ (k_p = 100 kN/m, k_e = 1000 kN/m, k_{ce} = 2000 kN/m, k_{cp} = 5 kN/m).

As it can be seen in Figure 5, by increasing the interface energy, the plastic work increases; however the elastic work is very small for the range of Γ investigated here and it does not change significantly with the interface energy. An increase in the interface energy increases the work of adhesion.

CONCLUSIONS

A new linear elasto-plastic and adhesive contact model for spherical particles has been proposed based on improvements of Luding's model [1] and considering aspects of Thornton and Ning's [2] and Tomas's [3] contact models. Plastic deformation of contacts during loading and pure elastic unloading, accompanied by adhesion are considered, for which the pull-off force increases with plastic deformation. Sensitivity analyses of the model parameters on work of compaction reveal that by increasing the stiffness ratio (k_e/k_p) the normalised plastic work increases and the normalised elastic work decreases. By increasing the interface energy, the plastic work increases, however the elastic work does not change. This highlights the flexibility of the model in representing a wide range of particulate materials. The linear nature of the model leads to time efficient simulations whilst still capturing the complex material behaviour.

REFERENCES

1. S. Luding, *Granular Matter* **10**, 235-246 (2008).
2. C. Thornton, Z. Ning, *Powder Technology* **99**, 154-162 (1998).
3. J. Tomas, *Granular Matter* **6**, 75-86 (2004).
4. K.L. Johnson, K. Kendall and A.D. Roberts Proceeding of the Royal Society A **324**, 178-189 (1971).
5. G.I. Tardos, S. Mcnamara and I. Talu, *Powder Technology* **131**, 23-39 (2003).